

LA-UR-17-31380

Approved for public release; distribution is unlimited.

Title: Failure Diameter Resolution Study

Author(s): Menikoff, Ralph

Intended for: Report

Issued: 2017-12-19



FAILURE DIAMETER RESOLUTION STUDY

RALPH MENIKOFF

December 4, 2017

Abstract

Previously the SURFplus reactive burn model was calibrated for the TATB based explosive PBX 9502. The calibration was based on fitting Pop plot data, the failure diameter and the limiting detonation speed, and curvature effect data for small curvature. The model failure diameter is determined utilizing 2-D simulations of an unconfined rate stick to find the minimum diameter for which a detonation wave propagates. Here we examine the effect of mesh resolution on an unconfined rate stick with a diameter (10 mm) slightly greater than the measured failure diameter (8 to 9 mm).

1 Introduction

The SURFplus is a reactive burn model for shock initiation and propagation of detonation waves in a high explosive. It is based on a fast hot-spot rate and a subsequent slow rate for the energy released as carbon clusters grow [Menikoff and Shaw, 2012]. Previously, the SURFplus model was calibrated for the TATB based explosive PBX 9502 [Menikoff, 2017b]. The calibration was based on fitting Pop plot data, the failure diameter and limiting detonation speed, and curvature effect data for small curvature. We use the same burn model (equations of state for reactants and products, and ambient 9502 rate parameters) for the simulations reported here.

The model failure diameter is determined utilizing 2-D simulations of an unconfined rate stick to find the minimum diameter for which a detonation wave propagates. The simulations used the Eulerian adaptive mesh resolution code xRage. The fast reaction zone was refined to a cell size of 0.016 mm. At this resolution, a planar underdriven detonation wave would have only 6 to 8 cells in the fast reaction zone and 20 to 30 % burn fraction in the lead shock rise. The fast reaction zone is important for the failure diameter simulations since the detonation front curvature results in the sonic point being near the end of the fast reaction. Hence the slow reaction does not contribute to driving the detonation wave.

Finer resolution requires a smaller time step and hence a longer run time for a simulation. Application simulations frequently use coarser resolution than used for the failure diameter calibration simulations. Past experience indicates that with coarse resolution curved detonation waves propagate at a slightly slower speed [Menikoff, 2014], and the numerical Pop plot shifts up in the run-to-detonation distances vs shock pressure plane, *i.e.*, the HE is less sensitive to shock initiation.

Here we examine the effect of mesh resolution on the failure diameter by running simulations with the fast reaction zone resolved 4 times finer (cell size of 0.004 mm) and 4 times coarser (cell size of 0.063 mm) than used for the calibration simulations. The new simulations are for a 10 mm diameter rate stick. This is slightly larger than the PBX 9502 failure diameter of 8 to 9 mm (depending on lot). It has the advantage that there is experimental data [Hill et al., 1998] that can be used to compare with the simulated detonation front shape. We will refer to the three resolutions as coarse, standard and very-fine.

Other simulations, which are not reported here, show that the failure diameter is slightly larger at the coarse resolution. In addition just above the failure diameter there are small fluctuations in the detonation speed as the wave propagates along the rate stick. The 10 mm diameter rate stick avoids these complication and allows for a better comparison of the simulated results at the different resolutions.

2 Numerical results

The setup for the rate stick simulations is described in §3.1 of [Menikoff, 2017a]. A long 10 mm diameter rate stick is initiated with a detonation wave in a 25 mm diameter rate stick. This slightly overdrives the narrower rate stick and leads to a prompt initiation in the 10 mm diameter rate stick we chose to study. With a length to diameter ratio of 5, there is sufficient run distance for the detonation wave to be nearly steady at the end of the run.

The detonation speed as a function of axial distance for the simulations is shown in fig. 1. After a transient of 2 to 3 diameters run distance, the nearly constant speed indicates that the detonation wave is close to steady. The figure shows that the detonation speed decreases as the cell size is increased. The speed at the coarse resolution is 0.6% less than at the very-fine resolution.

To put the variation of the simulated detonation speed in perspective, we note that the experimental detonation speed varies with lot. For a 10 mm diameter rate stick, the detonation speed is 7.475 km/s for lot 79-04 [Campbell, 1984] and 7.415 km/s for lot HOL88H891-008 [Hill et al., 1998]. The variation in detonation speed from mesh resolution is within the experimental variation due to lot. The very-fine simulation better agrees with the value from the calibration experiments [Campbell, 1984] than the coarser resolutions.

An important issue is how well the reaction region is resolved for a given cell size. From the previous calibration simulations, the lead shock pressure [Menikoff, 2017b, fig. 8] is highest on the axis ($\approx 37 \,\text{GPa}$) and decreases monotonically to the sonic pressure on the boundary ($\approx 14 \,\text{GPa}$);

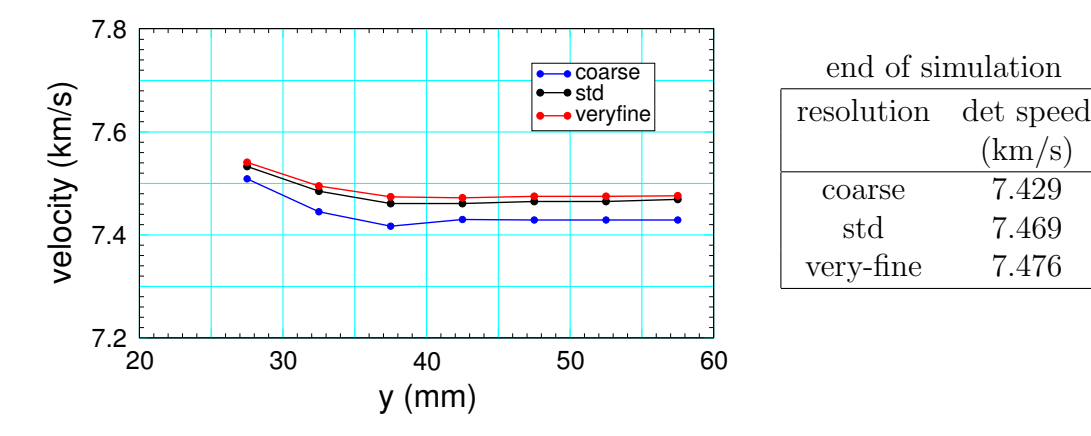


Figure 1: Detonation speed vs axial distance for simulations at coarse, standard and very-fine resolution. The 10 mm diameter rate stick extends from y = 15 to 65 mm. The detonation speed is based on probe points (numerical timing pins) on axis 5 mm apart.

see also fig. 3 below. This leads to a substantial variation (over an order of magnitude) of the burn rate with radius; see [Menikoff, 2017b, fig. 2].

Figure 2 shows profiles (on axis and near the boundary) of the pressure and reaction progress variables for the three resolutions. On the axis, at coarse resolution the pressure for the fast rate portion of the reaction zone is noticeably under-resolved with substantial reaction occurring in the lead shock profile. After the fast reaction, a few tenths of mm behind the shock front, for all three resolutions the pressure profiles are nearly the same. However, the front curvature results in the sonic point being near the end of the fast reaction. Consequently, the energy released by the fast reaction drives the detonation.

Near the boundary (radius within $0.5 \,\mathrm{mm}$), the shock pressure and hence the burn rate is sufficiently low that even at coarse resolution the pressure profile is well resolved. This is important because the front shape and the detonation speed is largely determine by the boundary condition for the rate stick; *i.e.*, the sonic pressure on the shock polar.

The detonation front shape and shock pressure along the front are shown in fig. 3 for the three resolutions. For later use in computing the front curvature, the discrete numerical front shapes were fit to an analytic function developed by Hill et al. [1998] for analyzing experimental data to determine the curvature effect. Several points are noteworthy. The front shapes, y(r), are relative to the position on the axis; i.e., y(0) = 0. The front position at fixed radius is monotonically increasing with finer resolution. Moreover, the front shapes from the simulations appear to be converging to the experimentally measured shape, with the very-fine resolution differing slightly near the boundary.

The shock pressure at fixed radius is also monotonically increasing with finer resolution and is likely to converge with further refinement. Two points are noteworthy for the coarse resolution simulations. Comparing with profiles in fig. 2, on the axis where there is substantial burning in the shock rise, the shock is detected in the shock profile one cell before the peak. This leads to a low shock pressure, and consequently lowers the burn rate. There is also numerical noise or small radial variations in the shock pressure. The amplitude of the variations is very much reduced at finer resolution.

Using the fits to the front shape shown in fig. 3, the front curvature and the detonation speed normal to the front can be calculated. The curvature as function of radius and $D_n(\kappa)$ are shown in fig. 4 for the three resolutions. The variation of $\kappa(r)$ with resolution is largest within 1 mm of the boundary where fig. 3 shows that the shock pressure P(r) is rapidly changing to meet the required sonic boundary pressure. The dependence of $D_n(\kappa)$ with resolution appears larger. This is in large part due to the sensitive of calculating D_n and κ from the front shape since they depend on the first and second derivatives; i.e., dy/dr and d^2y/dr^2 .

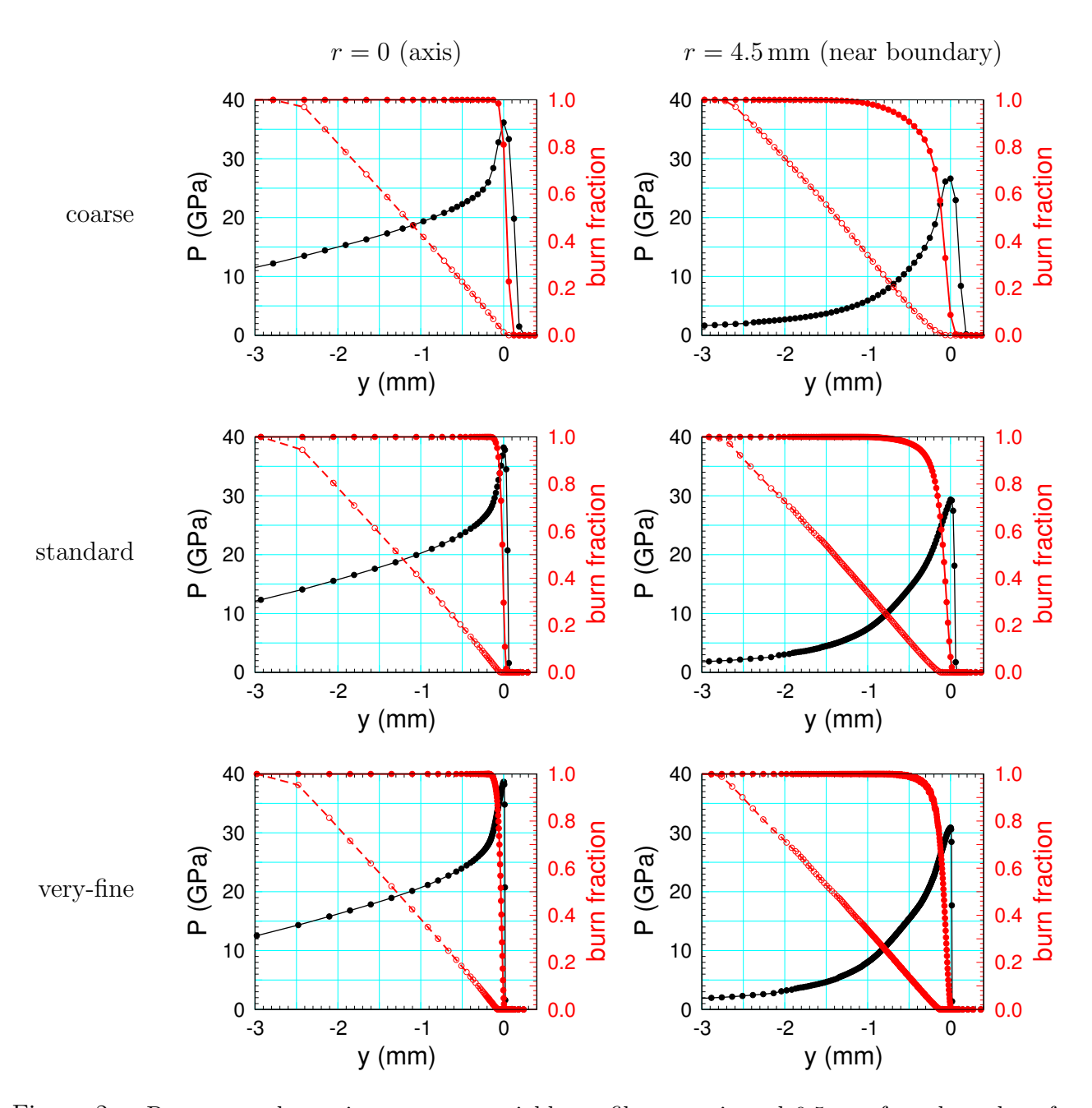


Figure 2: Pressure and reaction progress variable profiles on axis and 0.5 mm from boundary for 10 mm diameter rate stick; from simulations at coarse, standard and very-fine resolution. Symbols denote grid cells. Solid red circle for fast hot-spot rate and open red circle for slow carbon-clustering rate.

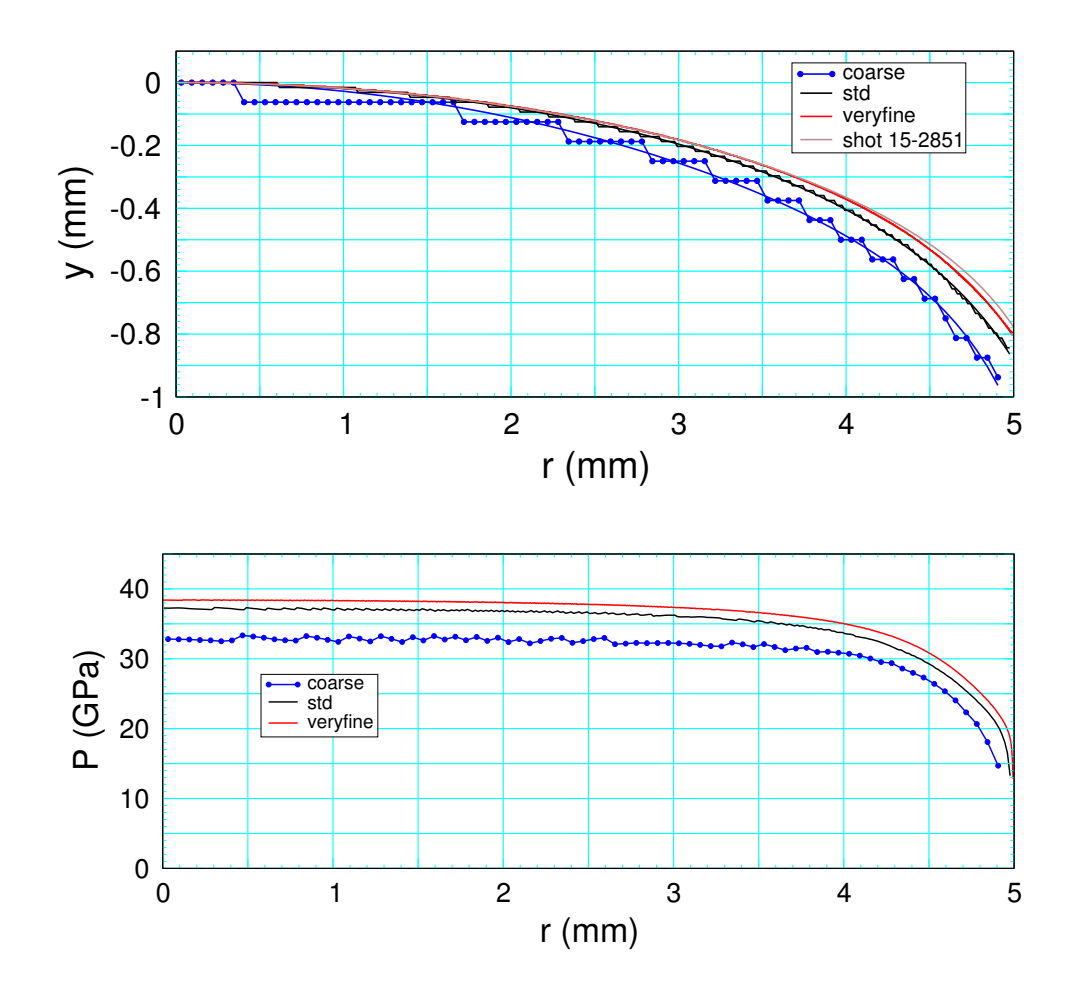


Figure 3: Front shape and lead shock pressure for 10 mm diameter rate stick. Experimental shape is for lot HOL88H891-008 from [Hill et al., 1998]. For the coarse mesh symbols denote grid cells. Stair-steps for the front shape result from discretization to cell centers. Smooth front shapes utilize fitting form developed by Hill et al. [1998].

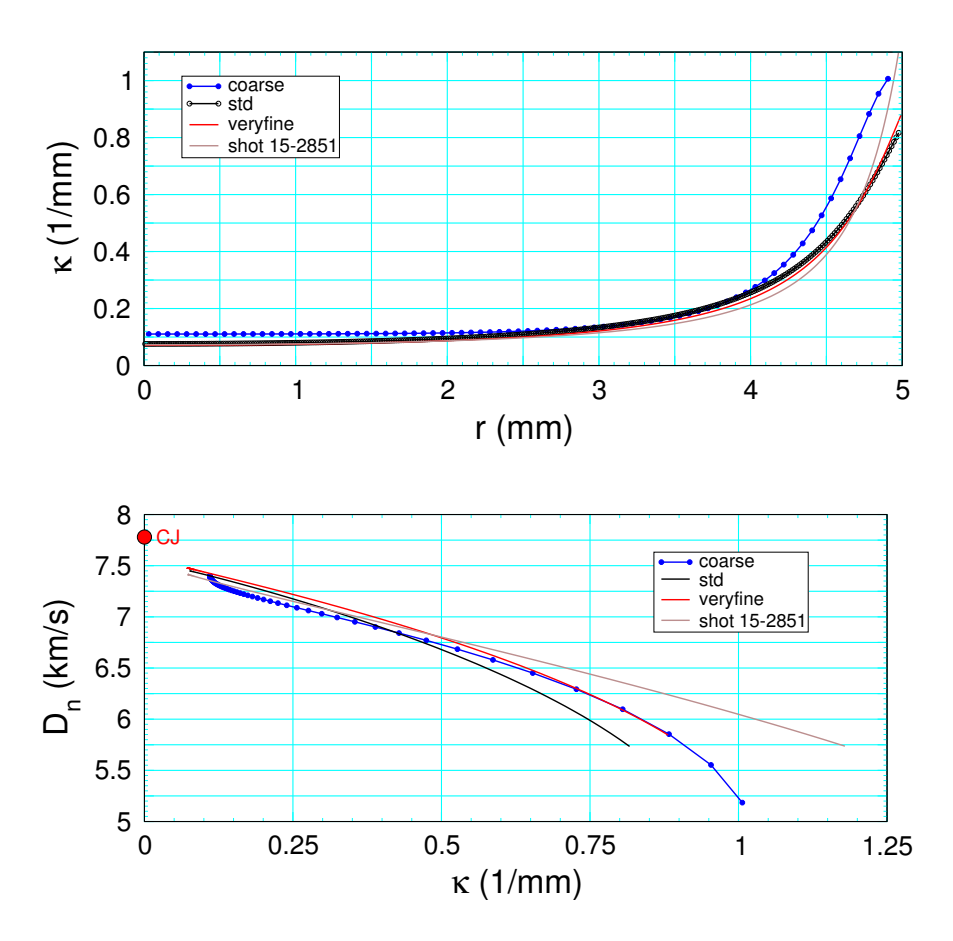


Figure 4: Front curvature as a function of radius and $D_n(\kappa)$ for 10 mm diameter rate stick. The experimental data is for lot HOL88H891-008 from [Hill et al., 1998]. For the coarse mesh symbols denote grid cells. Red symbol for the CJ detonation speed is based on the products EOS and the initial reactant state.

3 Summary

Simulations were run with the SURFplus reactive burn model in the xRage code for a detonation wave in a 10 mm diameter unconfined rate stick of PBX 9502 at three mesh resolutions; coarse, standard and very-fine. Adaptive mesh refinement enabled the part of the reaction-zone dominated by the fast hot-spot rate to be resolved with 16, 64 and 256 cells per mm for the three resolutions. The standard resolution was previously used to calibrate the burn rate. The calibration included matching the failure diameter and the limiting detonation speed just above the failure diameter. The 10 mm diameter rate stick is slightly above the failure diameter of 8 to 9 mm.

Several quantities can be compared. On the coarse mesh the detonation speed is 0.6% lower than the value obtained on the very-fine mesh; see fig. 1. A simple measure of the front shape is the difference between the position on the axis and the boundary. The experimental value is 0.78 mm, and for the simulations 0.80, 0.86 and 0.96 mm for the very-fine, standard and coarse, respectively; see fig. 3. The shock pressure on axis was 38.4, 37.5 and 32.8 GPa for the very-fine, standard and coarse, respectively. The low value for the coarse resolution is mostly due to burning in the shock rise resulting in the shock detector algorithm picking the shock front 1 cell before the maximum pressure, which should be the shock pressure.

The calculated front curvature as a function of radius shown in fig. 4 are in good agreement for the standard and very-fine resolution simulations. They differ significantly from the experimental value within 0.5 mm of the boundary. The coarse simulation has a noticeably higher curvature. The difference for the curvature effect $D_n(\kappa)$ is somewhat large. This is due to κ depending on the second derivative of the front shape and the sensitivity to small variations in y(r). This implies that the numerical value of $D_n(\kappa)$ from a rate stick simulation would not be a good quantity to use in calibrating the burn model.

We note that the boundary shock pressure that affects the failure diameter is also likely to dominate dead zones from corner turning. For applications of this sort the standard resolution or better would be needed.

The computational cost for the three simulations is shown in table 1. The very-fine mesh requires significantly more run time even when more processors are used. If only the detonation speed were important for an application then there would be an advantage to calibrating model parameters with simulations on a coarse mesh.

Table 1: Variation of computational cost with resolution.

resolution	processors	run time
coarse	32	0.5 hr
std	32	2.6 hr
very-fine	128	10.3 hr

4 Added note

Simulations were run with two additional resolutions; coarser with fast reaction cell size of 0.125 mm, and very-coarse with cell size to 0.25 mm. With both of these resolutions the detonation wave on axis is captured in the sense of a shock capturing algorithm. That is, the numerical wave profile is artificial. It corresponds to a reactive shock and does not reflect the model rate.

Figure 5 shows the detonation speed along the axis for the expanded set of simulations. With the coarser resolution, the detonation speed decreases further; 2.5 % less than the value for the very fine resolution. The coarser resolution simulation is semi-quantitative largely because the fast rate is resolved near the rate stick boundary due to the lower rate for the boundary shock pressure.

At the very-coarse resolution, the detonation failed to propagate; *i.e.*, 10 mm was below the numerical failure diameter. Thus, for some applications, insufficient resolution may make a dramatic difference.

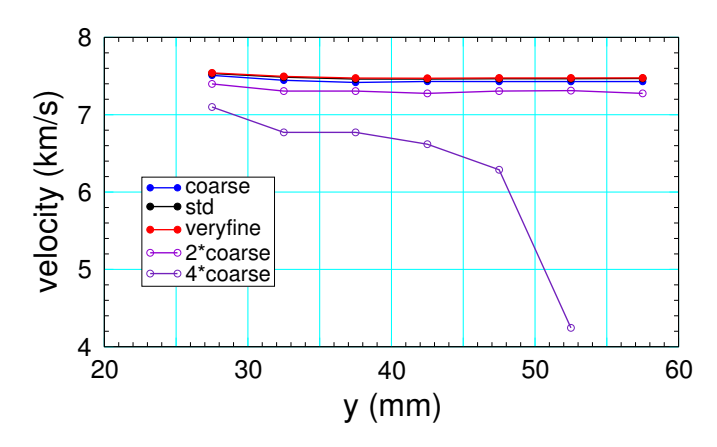


Figure 5: Detonation speed vs axial distance for simulations with 2 additional coarser resolutions. For the 4*coarse resolution the detonation wave failed to propagate; *i.e.*, 10 mm diameter rate stick is below the failure diameter for cell size of 0.25 mm.

References

- A. W. Campbell. Diameter effect and failure diameter of a TATB based explosive. *Propellants, Explosives, Pyrotechnics*, 9:183–187, 1984. URL http://dx.doi.org/10.1002/prep. 19840090602. 3
- L. G. Hill, J. B. Bdzil, and T. D. Aslam. Front curvature rate stick measurements and detonation shock dynamics calibration for PBX 9502 over a wide temperature range. In *Proceeding of the Eleventh International Symposium on Detonation*, pages 1029–1037, 1998. 2, 3, 4, 6, 7
- R. Menikoff. Effect of resolution on propagating detonation wave. Technical Report LA-UR-14-25140, Los Alamos National Laboratory, 2014. URL http://dx.doi.org/10.2172/1136940.
- R. Menikoff. Failure diameter of PBX 9502: Simulations with the SURFplus model. Technical Report LA-UR-17-25300, Los Alamos National Lab., 2017a. URL https://www.osti.gov/scitech/servlets/purl/1369155. 3
- R. Menikoff. SURFplus model calibration for PBX 9502. Technical Report LA-UR-17-31015, Los Alamos National Lab., 2017b. URL https://www.osti.gov/scitech/servlets/purl/1412839. 2, 3, 4
- R. Menikoff and M. S. Shaw. The SURF model and the curvature effect for PBX 9502. Combustion Theory And Modelling, pages 1140–1169, 2012. URL http://dx.doi.org/10.1080/13647830.2012.713994. 2